Biogeosciences Discuss., 9, 15633–15665, 2012
www.biogeosciences-discuss.net/9/15633/2012/
doi:10.5194/bgd-9-15633-2012

Biogeosciences Discussions

Ammonia emissions from beech forest after leaf fall – measurements and modelling

K. Hansen[1], L. L. Sørensen[2], O. Hertel[1,2], C. Geels[2], C. A. Skjøth[2,3], B. Jensen[2], and E. Boegh[1]

[1]Department of Environmental, Social and Spatial Change, Roskilde University, Roskilde, Denmark
[2]Department of Environmental Science, Aarhus University, Roskilde, Denmark
[3]Department of Physical Geography and Ecosystems Science, Lund University, Lund, Sweden

Received: 9 July 2012 – Accepted: 31 October 2012 – Published: 7 November 2012

Correspondence to: K. Hansen (krih@ruc.dk)

Published by Copernicus Publications on behalf of the European Geosciences Union.

Abstract

The understanding of biochemical feed-back mechanisms in the climate system is lacking knowledge in relation to bi-directional ammonia (NH_3) exchange between natural ecosystems and the atmosphere. We therefore study the atmospheric NH_3 fluxes during a 25 days period during autumn 2010 (21 October–15 November) for the Danish beech forest, Lille Bøgeskov, to address the hypothesis that NH_3 emissions occur from deciduous forests in relation to leaf fall. This is accomplished by using observations of vegetation status, NH_3 fluxes and model calculations. Vegetation status was observed using plant area index (PAI) and leaf area index (LAI). NH_3 fluxes were measured using the relaxed eddy accumulation (REA) method. The REA based NH_3 concentrations were compared to NH_3 denuder measurements. Model calculations were obtained with the Danish Ammonia MOdelling System (DAMOS). 57.7 % of the fluxes measured showed emission and 19.5 % showed deposition. The mean NH_3 flux was $0.087 \pm 0.19\,\mu g\,NH_3\text{-}N\,m^{-2}\,s^{-1}$. A clear tendency of the flux going from negative (deposition) to positive (emission) fluxes of up to $0.96 \pm 0.40\,\mu g\,NH_3\text{-}N\,m^{-2}\,s^{-1}$ throughout the measurement period was found. In the leaf fall period (23 October–8 November), an increase in the atmospheric NH_3 concentrations was related to the increasing forest NH_3 flux. The modelled concentration from DAMOS fits well the measured concentrations before leaf fall. During and after leaf fall, the modelled concentrations are too low. The results indicate that the missing contribution to atmospheric NH_3 concentration from vegetative surfaces related to leaf fall are of a relatively large magnitude. We therefore conclude that emissions from deciduous forests are important to include in model calculations of atmospheric NH_3 for forest ecosystems. Finally, diurnal variations in the measured NH_3 concentrations were related to meteorological conditions, forest phenology and the spatial distribution of local anthropogenic NH_3 sources. This suggests that an accurate description of ammonia fluxes over forest ecosystems requires a dynamic description of atmospheric and vegetation processes.

1 Introduction

Atmospheric ammonia (NH_3) plays an important role in air quality and critical load studies of natural and semi-natural ecosystems. NH_3 is a reactive nitrogen compound (N_r), which contributes to the formation of ammonium aerosols (NH_4^+) through atmospheric chemical reactions (Hertel et al., 2012a) and is leading to deposition to terrestrial and marine ecosystems (de Leeuw et al., 2003; Duce et al., 2008; Massad et al., 2010; Zhang et al., 2010). An enhanced load of N_r in terrestrial ecosystems can increase the rate of acidification and eutrophication processes and thereby reduce biodiversity and increase ecosystem vulnerability to extreme weather and insect attacks (Bobbink et al., 2010; Erisman et al., 2007; Stevens et al., 2004; Sutton et al., 2011; Xiankai et al., 2008). In nutrient limited ecosystems, N-deposition can also work to increase the C-sequestration and growth of vegetation (de Vries et al., 2009).

Budgets of atmospheric NH_3 for water and land areas are being carried out using atmospheric models (e.g. Bartnicki et al., 2011; de Leeuw et al., 2003; Geels et al., 2012a; Hertel et al., 2003; Langner et al., 2009). Model calculations indicate that particular forest ecosystems are exposed to critical load exceedances of nitrogen (Geels et al., 2012b; Hertel et al., 2012b). Generally the understanding of major biochemical feed-back mechanisms in the terrestrial climate system suffers from large uncertainties (Arneth et al., 2010) and lacking knowledge of the two-way (bi-directional) NH_3 exchange between the land/water surface and the atmosphere (Massad et al., 2010). Because natural NH_3 emissions have been assessed to a rather limited extent (Massad et al., 2010; Nemitz et al., 2001), they are not yet included in operational air pollution models (Menut and Bessagnet 2010).

Field studies showed that the deposition velocity of NH_3 for forests is relatively high and variable (Andersen et al., 1999; Duyzer et al., 1994; Wyers et al., 1992) and thereby complicating the understanding of forest NH_3 exchange processes and making model validation difficult. High deposition velocities for forests were simulated by four inferential models used across European sites, but large differences (up to factor 3) were

found between model results (Flechard et al., 2011). To achieve an improved understanding of the ecosystem-atmosphere NH_3 exchange processes, more datasets on NH_3 fluxes for ecosystems are needed.

Sources of atmospheric NH_3 are conceptually considered to be anthropogenic (e.g. Gyldenkærne et al., 2005; Hertel et al., 2012a) and primarily related to agricultural activities (e.g. Bouwman et al., 1997; Reis et al., 2009). In Europe, agricultural emissions arise from farm buildings (34–43 %), manure (22–26 %), fertilizers (17–26 %) and grazing animals (6–10 %) (Skjøth and Geels, 2012). Open water areas (e.g. Barrett, 1998; Sorensen et al., 2003) and natural land areas (e.g. Duyzer et al., 1994) have also been shown to emit NH_3. NH_3 emissions from forests are generally not included in official emission inventories (Reis et al., 2009) or the more detailed national inventories (Gyldenkærne et al., 2005; Velthof et al., 2012). However, NH_3 flux studies of forests indicate bi-directional flux patterns for NH_3 (Andersen et al., 1999, Erisman and Wyers, 1993; Sutton et al., 1997; Wyers and Erisman, 1998). Emissions of NH_3 from ecosystems are found to take place when the atmospheric NH_3 concentration is lower than the stomatal NH_3 compensation point (Kruit et al., 2007; Mattsson et al., 2009; Schjoerring et al., 1998) and from decomposing leaf litter (David et al., 2009; Nemitz et al., 2000a). Wang et al. (2011) discovered a seasonal dependence of the NH_3 compensation points of beech leaves and found largest emission potential in relation to the late senescent leaves. The effects of leaf NH_3 emissions in relation to leaf fall still remain to be quantified, particularly at canopy scale.

The main objective of this paper was to assess the NH_3 flux F_{NH_3} for a Danish deciduous forest in the leaf senescence period using high-resolution atmospheric measurements and local-scale concentration-deposition modelling. We investigate the hypothesis that NH_3 emissions occur from deciduous forests in relation to leaf fall by correlating this with NH_3 emissions and explore the importance of including such emissions in models. To do this, half-hourly measurements of F_{NH_3} were conducted using the Relaxed Eddy Accumulation (REA) technique for a Danish beech forest site in the

leaf fall period 21 October–15 November 2010 (Fig. 1) and compared to model calculations using the DAMOS modelling system.

2 Methods

2.1 Field site

The field station (Lille Bøgeskov) is located in the central part of Zealand (55°29′13″ N, 11°38′45″ E). Lille Bøgeskov extends approximately 1 km east-west and 2.5 km north-south with the field station located in the centre of the forest (Fig. 1). The field station includes a flux tower (57 m) and a scaffolding tower (24 m). The forest consists predominantly of 82-year-old beech trees (Fagus sylvatica) with an average canopy height of 26 m. Scattered stands of conifers constitute about 20 % of the forest area. The mean summer peak of LAI has been measured to be 4.6 since year 2000 with maximum LAI just above 5 (Pilegaard et al., 2011). Defoliation was observed to begin 23 October 2010 and leaf fall ended 8 November 2010. The surrounding landscape was primarily characterized by agricultural activities.

2.2 Leaf area index

In order to relate the atmospheric data to forest development, the plant area index (PAI) was measured during the growing season (May–November) continuous every 14–30 days using the LAI-2000 Plant Canopy Analyzer (LAI-2000 PCA). PAI was estimated using one above-canopy reading and 10 below-canopy readings conducted along an 18 m transect. The above-canopy readings were performed outside the forest edge. Measurements were made during uniformly overcast sky conditions, as recommended by the manufacturer. A 270° view cap was used to mask out shading from the operator. In order to assess the green leaf area index (LAI) from the PAI measurements, observations of leaf defoliation and leaf fall were used to adjust the data by linear interpolation to zero LAI at the time when there were no more green leaves present.

The uncertainty of measurements was calculated as the standard deviation of the 10 below-canopy readings.

2.3 Local meteorological measurements

The wind components in x-, y- and z-directions were measured at 10 Hz sampling using an ultra-sonic anemometer (Metek-uSonic-3 Scientific) installed above the forest canopy at 34 m height. Half-hourly averaged values of wind velocity, wind direction, friction velocity, temperature, and Monin Obukhov Length were conducted from the 10 Hz sampling. Measurements of global radiation, relative humidity, precipitation, soil water content and soil temperature were obtained from the European Fluxes Database Cluster (http://www.europe-fluxdata.eu).

2.4 Ammonia flux measurements

2.4.1 Relaxed eddy accumulation (REA)

The vertical turbulence driven flux of NH_3 was estimated using the REA technique (Businger and Oncley, 1990). REA simplifies the eddy accumulation methods (Hicks and Mcmillen, 1984), where the sampling speed must be proportional to the vertical wind velocity, by relaxing the sampling at a constant flow rate (Businger and Oncley, 1990). REA is based on the micrometeorological relationship between the vertical flux density F and the difference between the average trace gas concentration of upward and downward moving eddies. The vertical flux was obtained from Eq. (1):

$$F = b\,\sigma_w\,(C\uparrow - C\downarrow) \quad (1)$$

$C\uparrow$ and $C\downarrow$ are the average concentration in the up- and downdrafts respectively, σ_w is the standard deviation of the vertical wind velocity w', and b is a proportionality coefficient to be determined by the probability distribution of w, a dead-band width and the sampling height (Businger and Oncley 1990). The b-coefficient is well defined for an

ideal Gaussian joint frequency distribution of w and C. However turbulent transport, especially over very rough surfaces, often violates the underlying assumption of a linear relationship between w and C, (Ruppert et al., 2006), thus the use of a b-coefficient determined from a proxy scalar better reflects the correct b-coefficient for a certain measurement period. To increase the difference in $C\uparrow$ and $C\downarrow$ a dead-band was introduced (Businger and Oncley 1990) where sampling only took place when the vertical wind velocity exceeded a certain dead-band velocity w_0. The b-coefficient has to be corrected for the choice of dead-band velocity:

$$b = b_0 \exp \frac{-0.75 \cdot w_0}{\sigma_w} \quad (2)$$

w_0 is the dynamic dead-band (sat to 0.5 σ_w m s^{-1} in this study), b_0 is the coefficient when $w_0 = 0$ and b_0 was calculated based on the vertical heat flux:

$$b_0 = \frac{T_{\text{flux}}}{\sigma_w \cdot (T\uparrow - T\downarrow)} \quad (3)$$

T_{flux} is the vertical heat flux, $T\uparrow$ and $T\downarrow$ are the temperature when the fluctuating component of w respectively is upward and downward directed. According to the theoretical principles of the REA method, b_0 shall be a value close to 0.4–0.6. Therefore a criterion that asserts if b_0 is less that 0.2 or higher than 0.8, then b_0 =0.6 was used (Oncley et al., 1993).

A system to measure canopy-scale F_{NH_3} (µg NH_3-N m^{-2} s^{-1}) based on the REA technique was employed in the flux tower at the forest field station (Fig. 2). The system consisted of three parts; (1) a sonic anemometer measuring vertical wind speed, (2) an inlet system, and (3) an analytical detection system to detect the concentration signals (Fig. 3). The sonic anemometer was located in the mast in a height of 34 m to control the conditional sampling of atmospheric NH_3 in the up- and downdrafts respectively. The inlet system, comprised by two Wet Effluent Diffusion Denuders (WEDDs),

was located just below the sonic anemometer in 33 m. The WEDDs collected atmospheric NH_3 from upward and downward eddies separately by diffusion into a water film (Hensen et al., 2009). The aqueous NH_3 solution from the two WEDDs was pumped with a constant flow directly to the analytical detection system which was located at the top floor of a scaffolding tower. A fluorescent compound was produced by mixing *o*-phthaldialdehyde (OPA), sulphite, and the aqueous NH_3 solution (Sorensen et al., 1994). The liquid was heated to 60 °C to enhance the formation of the fluorescent compound before injection into the fluorescence detector. Detailed information of the WEDD and the analytical system can be found in Sorensen et al. (1994). To prevent freezing of the fluent when air temperature was near freezing point, the water was mixed with ethanol. The analytical system was calibrated using standard calibration fluids of 0, 10 and 25 ppb NH_3. The REA system was running from 21 October to 15 November 2010 with two short breaks due to technical work on the instruments (two hours on 1 November and three days from 5 to 8 November). Half-hourly estimates of F_{NH_3} were calculated from Eq. (1).

The uncertainty of measurements and detection limit was determined from standard deviation between several calibration measurements of 25 ppb and 0 ppb concentration liquids respectively both on the WEDD up and WEDD down. A larger measurement uncertainty was related to the sub-system sampling the downdraft eddies (0.6916 µg NH_3-N m^{-3}) than to the updraft sub-system (0.0085 µg NH_3-N m^{-3}). For a few measurements on 25 October, estimates of the half-hourly mean concentration c_{RNH_3} (µg NH_3-N m^{-3}) are lower than the actual limit of detection (0.03 µg NH_3-N m^{-3}). The REA system requires constant flows of air and liquids in the system to give correct concentration and flux estimates. The reliability of these measurements was assessed by comparing c_{RNH_3} to atmospheric NH_3 concentration measurements from diffusion denuders (c_{dNH_3}).

2.5 Denuder measurement

Atmospheric NH_3 concentration c_{dNH_3} ($\mu g\, NH_3\text{-}N\, m^{-3}$) in 29.8 m height (Fig. 2) was sampled using seven glass diffusion denuders (15 cm long) for the period 26 October–11 November for comparison with the measured REA NH_3 concentration (c_{RNH_3}). The denuders were coated with a solution of citric acid in methanol which effectively captures NH_3. Air was pumped through the denuders at 300 ml min^{-1}. Chemical analyses of denuders were performed using ion chromatography. The uncertainty of measurements was estimated as the standard deviation of the three denuders, and the detection limit was calculated as 3 times the standard deviation of the unexposed denuders (blank) to be 0.003 $\mu g\, NH_3\text{-}N\, m^{-3}$, following the method used by Andersen et al. (1999).

An uncertainty related to the comparison of atmospheric NH_3 concentration measurements in two different heights (c_{RNH_3} in 33 m and c_{dNH_3} in 29.8 m) must be expected. However, previous atmospheric NH_3 profile measurements above a spruce forest in Denmark, showed only little difference over 8 m in the NH_3 the concentration (Andersen et al. 1999).

2.6 Model calculations using DAMOS

The atmospheric NH_3 deposition was modelled using the DAMOS system (Geels et al., 2012b). DAMOS is a combination of the regional scale DEHM model (Brandt et al., 2012; Christensen, 1997) and the local-scale Gaussian dispersion-deposition model OML-DEP (Sommer et al., 2009). DEHM includes a detailed NH_3 emission model (Gyldenkærne et al., 2005; Skjøth et al., 2004, 2011) and provided in this study the wet NH_3 deposition and upwind boundary conditions for the local-scale OML-DEP model. OML-DEP was used to simulate atmospheric NH_3 concentrations and deposition rates using a one-way dry deposition scheme (Simpson et al., 2003), a high spatial resolution (100 m) land cover (Nielsen et al., 2000) and local field NH_3 emissions (Gyldenkærne et al., 2005; Skjøth et al., 2004). Estimates of field emissions considered the annual animal production in each agricultural building, and the location of buildings

and storage facilities were represented by their geographical coordinates (Fig. 4). Temporal changes of emissions due to variable meteorological conditions, particularly air temperature and length of local growing season were also taken into account (Skjøth et al., 2004, 2011). OML-DEP provided hourly simulations throughout the measurement period for 40 × 40 receptor points in a 16 km × 16 km grid. The flux tower was located in the centre of the modelling domain. DAMOS has for a number of years been used in the Danish atmospheric monitoring programme (e.g. Ellermann et al., 2010) and for assessing atmospheric N loads to sensitive ecosystems (Hertel et al., 2012b). A full description of DAMOS can be found in Geels et al. (2012b) and Hertel et al. (2012b).

3 Results

3.1 Meteorological and soil observations

The meteorological and soil conditions in the flux measurement period (21 October–15 November) are presented in Fig. 5. A series of frontal passages characterized the environmental conditions which caused winds to primarily originate from the west and south-west although interrupted by shorter periods of northerly winds between the 1–2 and 8–9 November (Fig. 5a). The friction velocity varied mainly between 0 and 1 m s^{-1}. However, during the period 3–14 November there were three episodes with u_* larger than 1 m s^{-1} caused by wind speeds of up to 8 m s^{-1} (Fig. 5b). The period with westerly winds were characterized by near neutral situations, while the shorter periods with more northerly winds had episodes with either stable or unstable conditions (Fig. 5f). Observed temperatures remained in the range 5–14 °C until 7 November, where after temperatures decreased and stabilized at 2–5 °C in the rest of the period (Fig. 5d). The same pattern was seen in soil temperature which decreased from 9 to 5 °C in the period (Fig. 5e). The period 21 October–7 November had episodes with a few mm of rain almost every day (Fig. 5g) which lead to high soil water content and high relative air humidity (Fig. 5i, h). From 8–14 November, it did not rain.

3.2 High-resolution ammonia fluxes

Figure 6 shows the measured NH_3 fluxes. F_{NH_3} varied from -0.33 ± 0.38 µg NH_3-N m^{-2} s^{-1} in the beginning of the measurement period to 0.96 ± 0.40 µg NH_3-N m^{-2} s^{-1} in the end of the period. The mean flux was 0.087 ± 0.19 µg NH_3-N m^{-2} s^{-1} (Table 1). A clear tendency of F_{NH_3} going from negative (deposition) to positive (emission) fluxes was seen throughout the measurement period. Even though estimates were related to large uncertainties (0.006–0.491 µg NH_3-N m^{-2} s^{-1} (Table 1)), the occurrence of emissions was convincing. Comparing LAI and F_{NH_3} during leaf fall showed a gradual increase of F_{NH_3} from negative to positive fluxes following defoliation (Fig. 6). When the green LAI reached zero (23 October), the deposition decreased towards zero (non-existent flux). In the transition period where senescent leaves and other plant material were still present in the canopy, but with decreasing LAI, F_{NH_3} gradually turned to positive fluxes, and a peak NH_3 emission of 0.72 µg NH_3-N m^{-2} s^{-1} was reached on 3 November. Following leaf fall which ended on 8 November, F_{NH_3} stayed positive, and three emission peaks (8–9, 10 and 12 November) of up to 0.96 ± 0.40 µg NH_3-N m^{-2} s^{-1} were observed.

3.3 Observed ammonia concentrations

Atmospheric NH_3 concentrations measured by the REA system (c_{RNH_3}) varied from less than 0.03 to 2 µg NH_3-N m^{-3} in the measurement period (Fig. 7). The mean c_{RNH_3} was 0.56 ± 0.35 µg NH_3-N m^{-3}, and the detection limit was found to be 0.03 µg NH_3-N m^{-3}. From 26 October to 11 November, the mean c_{RNH_3} was 0.68 ± 0.35 µg NH_3-N m^{-3}, and the mean concentration obtained from denuder measurements (c_{dNH_3}) was 0.67 ± 0.05 µg NH_3-N m^{-3} and above the detection limit (Table 2). A clear diurnal pattern was seen in c_{RNH_3} particularly in the beginning of the measurement period which indicated increasing c_{RNH_3} during night and decreasing c_{RNH_3} during daytime (Fig. 7).

The concentration rose (Fig. 4) indicate that the dominating contribution of atmospheric NH_3 originated from south-west where many smaller point sources were located, but the highest concentrations were related to north-westerly wind directions where two NH_3 point sources were located at the forest edge. Relatively low concentrations were seen when wind directions were north-east where only few NH_3 emission sources were located (Fig. 4).

3.4 Simulated ammonia concentration using DAMOS

Mean three-hourly modelled atmospheric concentrations by DAMOS (c_{mNH_3}) for the entire period (Fig. 7) varied between 0.03 ± 0.015 and 2.51 ± 1.255 µg NH_3-N m^{-3}, and mean c_{mNH_3} was 0.50 ± 0.25 µg NH_3-N m^{-3} (Table 2). It should be noted that the emission signal from the Danish area includes only point sources (stables and storage) as diffuse sources from agricultural areas are inactive in the period 1 October–1 February due to Danish legislations on fertilization management. This legislation on actual farming practice is dynamically incorporated in the NH_3 emission model. Apart from 5–6 peaks exceeding 1 µg NH_3-N m^{-3}, the simulated level of c_{mNH_3} remained between 0 and 1 µg NH_3-N m^{-3}, and no decreasing or increasing trends were observed for the period. The c_{mNH_3} peaks exceeding 1 µg NH_3-N m^{-3} (Fig. 7) were related mainly to contributions from local point sources located in the south-western sector (Fig. 4) and to difficulties of the model to handle low friction velocities and changes in atmospheric stability.

4 Discussion

Despite the different measurement heights of REA (33 m) and the denuders (29.8 m), the mean atmospheric NH_3 concentration measured for the period 26 October–11 November are in good agreement, i.e. 0.68 ± 0.35 (REA) and 0.67 ± 0.05 (Denuder), and the simulated concentrations are also in a comparable range, i.e.

0.56 ± 0.28 µg NH_3-N (DAMOS) (Table 2). These concentrations are comparable with measurements for forests in other Danish and US studies (Andersen et al., 1999; Pryor et al., 2001). Many studies have reported that forests generally act as efficient sinks taking up the atmospheric NH_3. In this study of only autumn months, 57.7 % of the measured fluxes indicated emissions and 19.5 % indicated depositions. The atmospheric ammonia flux measurements show an interesting temporal correlation with the canopy's vegetation development (Fig. 6) suggesting that deposition of NH_3 to the forest canopy decreases as LAI decreases, and that NH_3 emissions increase in the leaf fall period. Apart from decomposition of litter, natural emissions of NH_3 linked to the leaf stomatal compensation point may cause NH_3 emissions to increase in the senescent period (Wang et al., 2011). However such processes are not yet taken into account in the DAMOS system, and thus impacts of forest NH_3 emissions are not represented in the c_{NH_3} model calculations. The relations between the NH_3 emissions and vegetation status and other dynamics are discussed in the following along with the model performance.

4.1 LAI and NH_3 fluxes in the leaf fall period

Before 30 October 2010, the measured c_{RNH_3} was less than 0.5 µ,g NH_3-N m^{-3} and during the leaf fall period (23 October–8 November) a clear increase in the c_{RNH_3} is seen (Fig. 7). After 30 October, the c_{RNH_3} level was typical higher than the mean (0.56 ± 0.35 µg NH_3-N m^{-3}) for the measurement period. This increase was found to be related to the increasing forest NH_3 flux that was observed after 2 November (Fig. 6). The modelled concentration c_{mNH_3} did not show such increase in the same period indicating that a natural source, the forest, was causing the increase in c_{RNH_3}. After LAI reached zero, F_{NH_3} turns positive and changes from showing net deposition to net emissions of NH_3. The decreasing net deposition in the senescence period may be related to a reduced uptake of NH_3 through stomata and a smaller cuticular area for direct deposition along with a larger NH_3 emissions potential $\Gamma = [NH_4^+]/[H^+]$ of the

senescent leaves in the canopy related to remobilization during leaf senescence, likely to what Wang et al. (2011) found. Studies based on dynamic chamber techniques and within-canopy profile measurements of the NH_3 flux have reported NH_3 emissions from intensively managed ecosystems, and suggest re-emission from senescent leaves and decomposition of leaf litter to be a strong source of NH_3 emissions, particularly in humid conditions (David et al., 2009; Nemitz et al., 2000a). The emission potential for senescent leaves or leaf litter of grassland was studied in the GRAMINAE Integrated Experiment (Sutton et al., 2009) and reported by David et al. (2009) who found that Γ was a hundred times larger than that of green leaves, and that emissions were larger when the litter was moisturised than dry. Additionally, soil conditions such as temperature, moisture, pH, and N content has been found to be controlling factors for the NH_3 emissions (Riedo et al., 2002; Roelle and Aneja, 2002; Walker et al., 2012), however, not at crucial as the leaf litter. In this study, four evident emission peaks (2–4, 8–9, 10–11 and 12–14 November) are occurring of which three follow the leaf fall period (PAI = 0) (Fig. 6). Clear relations to the friction velocity (Fig. 5b) are seen for all four peak emissions indicating that the turbulent flow above the forest canopy controls a large part of the emission flux. No clear control pattern of other environmental or climatic conditions is seen that can explain the emissions, however, as precipitation occurred in a large part of the period (Fig. 5g), the emissions can be caused by evaporation of NH_3 from moist soil and wet leaves, as suggested by Pryor et al. (2001). The emissions found on 2–4 and 12–14 November were related to precipitation events followed by dry periods with relatively high air temperatures. Such conditions enhance the decomposition process of plant material and may explain the emissions on these occasions. Such conditions were not present on 8–9 and 10–11 November where peak emissions were also measured. Beside the forest's phenology, variations in meteorological and soil conditions influence the atmosphere-forest exchange of NH_3 through complex mechanisms of the physical, biological and chemical exchange mechanisms which are controlling the exchange processes (Flechard and Fowler, 1998; Pryor et al., 2001).

4.2 Model results

The simulated NH_3 concentration level in the senescent period fitted well the measured concentrations, but the modelled concentrations were too low following leaf fall (Fig. 7). On 10 November the measured c_{RNH_3} increased rapidly up to 1.98 µg NH_3-N m^{-3} caused by the forest NH_3 flux while the modelled c_{mNH_3} showed two narrow peaks that were related to changes in the atmospheric stability from the meteorological input to the model. c_{RNH_3} was twice the magnitude of c_{mNH_3} in this period, indicating that the missing contribution to c_{NH_3} from the forest is of a relatively large magnitude and therefore important to study and also include in model calculations.

Inadequate descriptions of surface properties such as aerodynamic roughness, stomatal resistance and processes related to the bi-directionality of atmospheric NH_3 fluxes represents uncertainties in current biosphere-atmosphere exchange modelling of NH_3 (Simpson et al., 2011). The complex mechanisms controlling these exchange processes make current model parameterisations of biological and chemical pathways and processes being empirical and based on few existing datasets (Flechard et al., 2011; Menut and Bessagnet, 2010; Pouliot et al., 2012). In DAMOS, the deposition is calculated for various land use categories and the surface resistance is divided into stomatal and non-stomatal components. For NH_3 the non-stomatal component includes, among other things, an acidity ratio between SO_2 and NH_3 (Emberson et al., 2000; Simpson et al., 2003), while a stomatal compensation point is not included. Many on-going studies search methods to include these processes in models to calculate the NH_3 exchange between vegetative surfaces and the atmosphere (Kruit et al., 2012; Massad et al., 2010). Riedo et al. (2002) coupled a two-layer resistance model to a NH_3 exchange model to include ecosystem N dynamics for an intensively managed grass land. The model, PaSim, was able to simulate effects of cutting and fertilization, but postulated that leaf litter was the reason for underestimation of NH_3 emission peaks. Other modelling concepts simulated leaf NH_3 emissions by including the stomatal compensation point and a litter layer with the emission potential, Γ, being

dependent on the relative air humidity (Nemitz et al., 2000b). Despite these efforts, we are still lacking knowledge of most biosphere-atmosphere exchange processes of N compounds (including potential feed-back mechanisms) (Arneth et al., 2010). Flux-studies in combination with model calculations are therefore needed in order to highlight the knowledge gabs and target future model improvements.

4.3 Diurnal dynamics in atmospheric ammonia

Measured c_{RNH_3} indicated clear diurnal pattern in the beginning of the measurement period with increased concentrations during night and decreased concentrations during day, showing that c_{NH_3} varied significantly over shorter time scales (Fig. 7). Stable atmospheric conditions during night time suppress the mixing of air and reduce the atmospheric boundary layer height, thereby leading to higher NH_3 concentrations in the lower atmosphere. The model did only capture these diurnal variations to a low extent (24–26 October) before LAI reached zero, and it even showed anti-correlations for the three days 21–24 October. It is known that Gaussian models including OML have problems when meteorological conditions change from stable to unstable and low friction velocities prevail (Olesen et al., 2007). In the current study, the comparison with high-resolution measurements showed that the observed diurnal variation c_{RNH_3} is hard to capture by the model. Some of the conceptual limitations can be improved with more advanced parameterisations such as updating the description of horizontal dispersion in OML. Other limitations require that the Gaussian OML is replaced with more advanced models (Olesen et al., 2007). The lower performance of OML during these few and special meteorological conditions does not affect the main conclusions: That there is a need to represent NH_3 releases from natural ecosystems, such as forests during leaf fall, for accurate high-spatial and high-temporal (diurnal) atmospheric simulation of c_{NH_3}. Therefore, more data on NH_3 fluxes are necessary for improving our understanding of controlling parameters in the biosphere-atmosphere NH_3 exchange processes.

5 Conclusions

Measurements showed that F_{NH_3} changed from negative (deposition) to positive (emission) fluxes during the period 21 October–15 November 2010 causing increased atmospheric NH_3 concentration. This change was temporally correlated to the vegetation status of the forest. The observations of LAI and PAI showed that the period with increased c_{NH_3} was in the leaf fall period and peak emissions up to 0.96 ± 0.40 µg NH_3-N m^{-2} s^{-1} were observed. The mean NH_3 concentrations were well simulated using DAMOS before leaf fall, but were underestimated following leaf fall. This points to the need for representing forest leaf fall and associated NH_3 emissions in chemical transport models, when simulating nitrogen-deposition to forests. These observations support the hypothesis that NH_3 emission occur from deciduous forests in relation to leaf fall. Additionally, diurnal variations of c_{NH_3} related to meteorological conditions (i.e. radiation control on stomatal resistance), forest phenology (i.e. LAI), and the spatial distribution of local anthropogenic NH_3 sources was found. This suggests that dedicated process studies including manipulation of ecosystems would be very valuable for improved understanding of NH_3 fluxes from natural vegetation. Despite large uncertainties associated with the results obtained in this study due to the assessment techniques and the limited dataset, the good agreement between c_{dNH_3}, c_{RNH_3} and c_{mNH_3} gives confidence in the data. The results must be considered as a good contribution to improve our understanding of the processes related to natural NH_3 emissions. This knowledge can be used in direct ecosystem manipulation studies or model studies in order to quantify the NH_3 emission flux from ecosystems and the total biosphere-atmosphere net flux of reactive nitrogen.

Acknowledgements. This study was conducted within the NitroEurope IP project (project no: 0174841-2). Additionally, the ECOCLIM project funded by the Danish Strategic Research Council with a PhD grant to Kristina Hansen, the EU project ECLAIRE (project no: 282910) and the Villum-Kann Rasmussen Foundation through a Post Doc grant to Carsten Ambelas Skjøth has supported this project financial. We gratefully acknowledge Helle V. Andersen and Christina F. Emborg (Dept. of Environmental Science, Aarhus University) for their making the chemical analyses of the denuder measurements.

References

Andersen, H. V., Hovmand, M. F., Hummelshøj, P., and Jensen, N. O.: Measurements of ammonia concentrations, fluxes and dry deposition velocities to a spruce forest 1991–1995, Atmos. Environ., 33, 1367–1383, doi:10.1016/S1352-2310(98)00363-X, 1999.

Arneth, A., Harrison, S. P., Zaehle, S., Tsigaridis, K., Menon, S., Bartlein, P. J., Feichter, J., Korhola, A., Kulmala, M., O'Donnell, D., Schurgers, G., Sorvari, S., and Vesala, T.: Terrestrial biogeochemical feedbacks in the climate system, Nat. Geosci., 3, 525–532, doi:10.1038/ngeo905, 2010.

Barrett, K.: Oceanic ammonia emissions in Europe and their transboundary fluxes, Atmos. Environ., 32, 381–391, doi:10.1016/S1352-2310(97)00279-3, 1998.

Bartnicki, J., Semeena, V. S., and Fagerli, H.: Atmospheric deposition of nitrogen to the Baltic Sea in the period 1995–2006, Atmos. Chem. Phys., 11, 10057–10069, doi:10.5194/acp-11-10057-2011, 2011.

Bobbink, R., Hicks, K., Galloway, J., Spranger, T., Alkemade, R., Ashmore, M., Bustamante, M., Cinderby, S., Davidson, E., Dentener, F., Emmett, B., Erisman, J.-W., Fenn, M., Gilliam, F., Nordin, A., Pardo, L., and De Vries, W.: Global assessment of nitrogen deposition effects on terrestrial plant diversity: a synthesis, Ecol. Appl., 20, 30–59, doi:10.1890/08-1140.1, 2010.

Bouwman, A., Lee, D., Asman, W., Dentener, F., VanderHoek, K., and Olivier, J.: A global high-resolution emission inventory for ammonia, Global Biochem. Cy., 11, 561–587, doi:10.1029/97GB02266, 1997.

Brandt, J., Silver, J. D., Frohn, L. M., Geels, C., Gross, A., Hansen, A. B., Hansen, K. H., Hedegaard, G. B., Skjøth, C. A., Villadsen, H., Zare, A., and Christensen, J. H.: An integrated model study for Europe and North America using the Danish Eulerian Hemispheric Model with focus on intercontinental transport of air pollution, Atmos. Environ., 53, 156–176, doi:10.1016/j.atmosenv.2012.01.011, 2012.

Businger, J. A. and Oncley, S. P.: Flux Measurement with Conditional Sampling, J. Atmos. Ocean. Technol., 7, 349–352, 1990.

Christensen, J. H.: The Danish Eulerian hemispheric model – A three-dimensional air pollution model used for the Arctic, Atmos. Environ., 31, 4169–4191, doi:10.1016/S1352-2310(97)00264-1, 1997.
David, M., Loubet, B., Cellier, P., Mattsson, M., Schjoerring, J. K., Nemitz, E., Roche, R., Riedo, M., and Sutton, M. A.: Ammonia sources and sinks in an intensively managed grassland canopy, Biogeosciences, 6, 1903–1915, doi:10.5194/bg-6-1903-2009, 2009.
de Leeuw, G., Spokes, L., Jickells, T., Skjoth, C., Hertel, O., Vignati, E., Tamm, S., Schulz, M., Sorensen, L., Pedersen, B., Klein, L., and Schlunzen, K.: Atmospheric nitrogen inputs into the North Sea: effect on productivity, Cont. Shelf Res., 23, 1743–1755, doi:10.1016/j.csr.2003.06.011, 2003.
de Vries, W., Solberg, S., Dobbertin, M., Sterba, H., Laubhann, D., van Oijen, M., Evans, C., Gundersen, P., Kros, J., Wamelink, G. W. W., Reinds, G. J., and Sutton, M. A.: The impact of nitrogen deposition on carbon sequestration by European forests and heathlands RID F-2087-2010 RID B-2192-2008, For. Ecol. Manage., 258, 1814–1823, doi:10.1016/j.foreco.2009.02.034, 2009.
Duce, R. A., LaRoche, J., Altieri, K., Arrigo, K. R., Baker, A. R., Capone, D. G., Cornell, S., Dentener, F., Galloway, J., Ganeshram, R. S., Geider, R. J., Jickells, T., Kuypers, M. M., Langlois, R., Liss, P. S., Liu, S. M., Middelburg, J. J., Moore, C. M., Nickovic, S., Oschlies, A., Pedersen, T., Prospero, J., Schlitzer, R., Seitzinger, S., Sorensen, L. L., Uematsu, M., Ulloa, O., Voss, M., Ward, B., and Zamora, L.: Impacts of atmospheric anthropogenic nitrogen on the open ocean, Science, 320, 893–897, doi:10.1126/science.1150369, 2008.
Duyzer, J., Verhagen, H. L. M., Weststrate, J. H., Bosveld, F. C., and Vermetten, A. W. M.: The Dry Deposition of Ammonia Onto A Douglas-Fir Forest in the Netherlands, Atmos. Environ., 28, 1241–1253, doi:10.1016/1352-2310(94)90271-2, 1994.
Ellermann, T., Andersen, H. V., Bossi, R., Christensen, J., Kemp, K., Løfstrøm, P., and Monies, C.: Atmospheric deposition 2008 NOVANA (In Danish: Atmosfærisk deposition 2008 NOVANA), National Environmental Research Institute, Aarhus University, 82 pp., 2010.
Emberson, L. D., Ashmore, M. R., Cambridge, H. M., Simpson, D., and Tuovinen, J. P.: Modelling stomatal ozone flux across Europe, Environ. Pollut., 109, 403–413, doi:10.1016/S0269-7491(00)00043-9, 2000.
Erisman, J. W. and Wyers, G. P.: Continuous Measurements of Surface Exchange of SO_2 and NH_3 – Implications for Their Possible Interaction in the Deposition Process, Atmos. Environ. Part A-General Topics, 27, 1937–1949, doi:10.1016/0960-1686(93)90266-2, 1993.

Erisman, J. W., Bleeker, A., Galloway, J., and Sutton, M. S.: Reduced nitrogen in ecology and the environment, Environ. Pollut., 150, 140–149, doi:10.1016/j.envpol.2007.06.033, 2007.
Flechard, C. R. and Fowler, D.: Atmospheric ammonia at a moorland site. I: The meteorological control of ambient ammonia concentrations and the influence of local sources, Q. J. R. Meteorol. Soc., 124, 733–757, doi:10.1256/smsqj.54704, 1998.
Flechard, C. R., Nemitz, E., Smith, R. I., Fowler, D., Vermeulen, A. T., Bleeker, A., Erisman, J. W., Simpson, D., Zhang, L., Tang, Y. S., and Sutton, M. A.: Dry deposition of reactive nitrogen to European ecosystems: a comparison of inferential models across the NitroEurope network, Atmos. Chem. Phys., 11, 2703–2728, doi:10.5194/acp-11-2703-2011, 2011.
Geels, C., Hansen, K. M., Christensen, J. H., Ambelas Skjøth, C., Ellermann, T., Hedegaard, G. B., Hertel, O., Frohn, L. M., Gross, A., and Brandt, J.: Projected change in atmospheric nitrogen deposition to the Baltic Sea towards 2020, Atmos. Chem. Phys., 12, 2615–2629, doi:10.5194/acp-12-2615-2012, 2012a.
Geels, C., Andersen, H. V., Ambelas Skjøth, C., Christensen, J. H., Ellermann, T., Løfstrøm, P., Gyldenærne, S., Brandt, J., Hansen, K. M., Frohn, L. M., and Hertel, O.: Improved modelling of atmospheric ammonia over Denmark using the coupled modelling system DAMOS, Biogeosciences, 9, 2625–2647, doi:10.5194/bg-9-2625-2012, 2012b.
Gyldenkærne, S., Skjøth, C. A., Hertel, O., and Ellermann, T.: A dynamical ammonia emission parameterization for use in air pollution models, J. Geophys. Res.-Atmos., 110, D07108, doi:10.1029/2004JD005459, 2005.
Hensen, A., Nemitz, E., Flynn, M. J., Blatter, A., Jones, S. K., Sørensen, L. L., Hensen, B., Pryor, S. C., Jensen, B., Otjes, R. P., Cobussen, J., Loubet, B., Erisman, J. W., Gallagher, M. W., Neftel, A., and Sutton, M. A.: Inter-comparison of ammonia fluxes obtained using the Relaxed Eddy Accumulation technique, Biogeosciences, 6, 2575–2588, doi:10.5194/bg-6-2575-2009, 2009.
Hertel, O., Ambelas Skjøth, C., Brandt, J., Christensen, J. H., Frohn, L. M., and Frydendall, J.: Operational mapping of atmospheric nitrogen deposition to the Baltic Sea, Atmos. Chem. Phys., 3, 2083–2099, doi:10.5194/acp-3-2083-2003, 2003.
Hertel, O., Skjøth, C. A., Reis, S., Bleeker, A., Harrison, R., Cape, J. N., Fowler, D., Skiba, U., Simpson, D., Jickells, T., Kulmala, M., Gyldenærne, S., Sørensen, L. L., Erisman, J. W., and Sutton, M. A.: Governing processes for reactive nitrogen compounds in the atmosphere in relation to ecosystem, climatic and human health impacts, Biogeosciences Discuss., 9, 9349–9423, doi:10.5194/bgd-9-9349-2012, 2012a.

Hertel, O., Geels, C., Frohn, L. M., Ellermann, T., Skjøth, C. A., Løfstrøm, P., Christensen, J. H., Andersen, H. V., and Peel, R. G.: Assessing atmospheric nitrogen deposition to natural and semi-natural ecosystems e Experience from Danish studies using the DAMOS, Atmos. Environ., 1–10, doi:10.1016/j.atmosenv.2012.02.071, in press, 2012b.

Hicks, B. B. and Mcmillen, R. T.: A Simulation of the Eddy Accumulation Method for Measuring Pollutant Fluxes, J. Clim. Appl. Meteorol., 23, 637–643, doi:10.1175/1520-0450(1984)023<0637:ASOTEA>2.0.CO;2, 1984.

Kruit, R. J. W., Schaap, M., Sauter, F. J., van Zanten, M. C., and van Pul, W. A. J.: Modeling the distribution of ammonia across Europe including bi-directional surface-atmosphere exchange, Biogeosciences Discuss., 9, 4877–4918, doi:10.5194/bgd-9-4877-2012, 2012.

Kruit, R. J. W., van Pul, W. A. J., Otjes, R. P., Hofschreuder, P., Jacobs, A. F. G., and Holtslag, A. A. M.: Ammonia fluxes and derived canopy compensation points over non-fertilized agricultural grassland in The Netherlands using the new gradient ammonia – high accuracy – monitor (GRAHAM), Atmos. Environ., 41, 1275–1287, 2007.

Langner, J., Andersson, C., and Engardt, M.: Atmospheric input of nitrogen to the Baltic Sea basin: present situation, variability due to meteorology and impact of climate change, Boreal Environ. Res., 14, 226–237, 2009.

Massad, R.-S., Nemitz, E., and Sutton, M. A.: Review and parameterisation of bi-directional ammonia exchange between vegetation and the atmosphere, Atmos. Chem. Phys., 10, 10359–10386, doi:10.5194/acp-10-10359-2010, 2010.

Mattsson, M., Herrmann, B., David, M., Loubet, B., Riedo, M., Theobald, M. R., Sutton, M. A., Bruhn, D., Neftel, A., and Schjoerring, J. K.: Temporal variability in bioassays of the stomatal ammonia compensation point in relation to plant and soil nitrogen parameters in intensively managed grassland, Biogeosciences, 6, 171–179, doi:10.5194/bg-6-171-2009, 2009.

Menut, L. and Bessagnet, B.: Atmospheric composition forecasting in Europe, Ann. Geophys., 28, 61–74, 2010,
http://www.ann-geophys.net/28/61/2010/.

Nemitz, E., Milford, C., and Sutton, M. A.: A two-layer canopy compensation point model for describing bi-directional biosphere-atmosphere exchange of ammonia, Q. J. R. Meteorol. Soc., 127, 815–833, doi:10.1256/smsqj.57305, 2001.

Nemitz, E., Sutton, M., Gut, A., San Jose, R., Husted, S., and Schjoerring, J.: Sources and sinks of ammonia within an oilseed rape canopy, Agric. For. Meteorol., 105, 385–404, doi:10.1016/S0168-1923(00)00205-7, 2000a.

Nemitz, E., Sutton, M., Schjoerring, J., Husted, S., and Wyers, G.: Resistance modelling of ammonia exchange over oilseed rape, Agric. For. Meteorol., 105, 405–425, doi:10.1016/S0168-1923(00)00206-9, 2000b.

Nielsen, K., Stjernholm, M., Olsen, B. O., Müller-Wohlfeil, D., Madsen, I. K.,A., Groom, G., Hansen, H. S., Rolev, A. M., Hermansen, B., Skov-Petersen, H., Johannsen, V. K., Hvidberg, M., Jensen, J. E., Bacher, V., and Larsen, H.: Areal Informations Systemet – AIS. Technical report, Danish Ministry of Environment, Denmark, 2000.

Olesen, H. R., Berkowicz, R. B., and Løfstrøm, P.: OML: Review of model formulation, National Environmental Research Institute, Denmark. NERI, Technical Report No. 609, 130 pp., 2007.

Oncley, S. P., Delany, A. C., Horst, T. W., and Tans, P. P.: Verification of Flux Measurement Using Relaxed Eddy Accumulation, Atmos. Env. Part A-General Topics, 27, 2417–2426, 1993.

Pilegaard, K., Ibrom, A., Courtney, M. S., Hummelshoj, P., and Jensen, N. O.: Increasing net CO_2 uptake by a Danish beech forest during the period from 1996 to 2009 RID A-9850-2011, Agric. For. Meteorol., 151, 934–946, doi:10.1016/j.agrformet.2011.02.013, 2011.

Pouliot, G., Pierce, T., van der Gon, H. D., Schaap, M., Moran, M., and Nopmongcol, U.: Comparing emission inventories and model-ready emission datasets between Europe and North America for the AQMEII project, Atmos. Environ., 53, 4–14, doi:10.1016/j.atmosenv.2011.12.041, 2012.

Pryor, S. C., Barthelmie, R. J., Sorensen, L. L., and Jensen, B.: Ammonia concentrations and fluxes over a forest in the midwestern USA, Atmos. Environ., 35, 5645–5656, doi:10.1016/S1352-2310(01)00259-X, 2001.

Reis, S., Pinder, R. W., Zhang, M., Lijie, G., and Sutton, M. A.: Reactive nitrogen in atmospheric emission inventories, Atmos. Chem. Phys., 9, 7657–7677, doi:10.5194/acp-9-7657-2009, 2009.

Riedo, M., Milford, C., Schmid, M., and Sutton, M.: Coupling soil-plant-atmosphere exchange of ammonia with ecosystem functioning in grasslands, Ecol. Model., 158, 83–110, doi:10.1016/S0304-3800(02)00169-2, 2002.

Roelle, P. A. and Aneja, V. P.: Characterization of ammonia emissions from soils in the upper coastal plain, North Carolina, Atmos. Environ., 36, 1087–1097, doi:10.1016/S1352-2310(01)00355-7, 2002.

Ruppert, J., Thomas, C., and Foken, T.: Scalar similarity for relaxed eddy accumulation methods, Bound. -Layer Meteorol., 120, 39–63, doi:10.1007/s10546-005-9043-3, 2006.

Schjoerring, J. K., Husted, S., and Mattsson, M.: Physiological parameters controlling plant-atmosphere ammonia exchange, Atmos. Environ., 32, 491–498, doi:10.1016/S1352-2310(97)00006-X, 1998.

Simpson, D., Fagerli, H., Jonson, J. E., Tsyro, S., Wind, P., and Tuovinen J-P: Transboundary Acidification, Eutrophication and Ground Level Ozone in Europe, PART I, Unified EMEP Model Description, 104 pp., 2003.

Simpson, D., Aas, W., Bartnicki, J., Berge, H., Bleeker, A., Cuvelier, K., Dentener, F., Dore, T., Erisman, J. W., Fagerli, H., Flechard, C., Hertel, O., Jaarsveld, H. v., Jenkin, M., Schaap, M., Semeena, V. S., Thunis, P., Vautard, R., and Vieno, M.: Atmospheric transport and deposition of nitrogen in Europe, in: The European Nitrogen Assessment: Sutton, M., Howard, C. M., Erisman, J. W., Billen, G., Bleeker, A., Grennfelt, P., Grinsven, H., and Grizzetti, B., Cambridge, University Press, 298–316, 2011.

Skjøth, C. A. and Geels, C.: The effect of climate and climate change on ammonia emissions in Europe, Atmos. Chem. Phys. Discuss., 12, 23403–23431, doi:10.5194/acpd-12-23403-2012, 2012.

Skjøth, C. A., Hertel, O., Gyldenkærne, S., and Ellermann, T.: Implementing a dynamical ammonia emission parameterization in the large-scale air pollution model ACDEP, J. Geophys. Res. -Atmos., 109, D06306, doi:10.1029/2003JD003895, 2004.

Skjøth, C. A., Geels, C., Berge, H., Gyldenærne, S., Fagerli, H., Ellermann, T., Frohn, L. M., Christensen, J., Hansen, K. M., Hansen, K., and Hertel, O.: Spatial and temporal variations in ammonia emissions – a freely accessible model code for Europe, Atmos. Chem. Phys., 11, 5221–5236, doi:10.5194/acp-11-5221-2011, 2011.

Sommer, S. G., Østergård, H. S., Løfstrøm, P., Andersen, H. V., and Jensen, L. S.: Validation of model calculation of ammonia deposition in the neighbourhood of a poultry farm using measured NH_3 concentrations and N deposition, Atmos. Environ., 43, 915–920, doi:10.1016/j.atmosenv.2008.10.045, 2009.

Sorensen, L. L., Granby, K., Nielsen, H., and Asman, W. A. H.: Diffusion Scrubber Technique Used for Measurements of Atmospheric Ammonia, Atmos. Environ., 28, 3637–3645, doi:10.1016/1352-2310(94)00189-R, 1994.

Sorensen, L., Hertel, O., Skjoth, C., Lund, M., and Pedersen, B.: Fluxes of ammonia in the coastal marine boundary layer, Atmos. Environ., 37, 167–177, doi:10.1016/S1352-2310(03)00247-4, 2003.

Stevens, C. J., Dise, N. B., Mountford, J. O., and Gowing, D. J.: Impact of nitrogen deposition on the species richness of grasslands, Science, 303, 1876–1879, doi:10.1126/science.1094678, 2004.

Sutton, M. A., Perthue, E., Fowler, D., Storetonwest, R. L., Cape, J. N., Arends, B. G., and Mols, J. J.: Vertical distribution and fluxes of ammonia at Great Dun Fell, Atmos. Environ., 31, 2615–2624, doi:10.1016/S1352-2310(96)00180-X, 1997.

Sutton, M. A., Nemitz, E., Theobald, M. R., Milford, C., Dorsey, J. R., Gallagher, M. W., Hensen, A., Jongejan, P. A. C., Erisman, J. W., Mattsson, M., Schjoerring, J. K., Cellier, P., Loubet, B., Roche, R., Neftel, A., Hermann, B., Jones, S. K., Lehman, B. E., Horvath, L., Weidinger, T., Rajkai, K., Burkhardt, J., Löpmeier, F. J., and Daemmgen, U.: Dynamics of ammonia exchange with cut grassland: strategy and implementation of the GRAMINAE Integrated Experiment, Biogeosciences, 6, 309–331, doi:10.5194/bg-6-309-2009, 2009.

Sutton, M. A., Oenema, O., Erisman, J. W., Leip, A., van Grinsven, H., and Winiwarter, W.: Too much of a good thing, Nature, 472, 159–161, doi:10.1038/472159a, 2011.

Velthof, G. L., van Bruggen, C., Groenestein, C. M., de Haan, B. J., Hoogeveen, M. W., and Huijsmans, J. F. M.: A model for inventory of ammonia emissions from agriculture in the Netherlands, Atmos. Environ., 46, 248–255, doi:10.1016/j.atmosenv.2011.09.075, 2012.

Walker, J. T., Jones, M. R., Bash, J. O., Myles, L., Meyers, T., Schwede, D., Herrick, J., Nemitz, E., and Robarge, W.: Processes of ammonia air-surface exchange in a fertilized Zea mays canopy, Biogeosciences Discuss., 9, 7893–7941, doi:10.5194/bgd-9-7893-2012, 2012.

Wang, L., Xu, Y., and Schjoerring, J. K.: Seasonal variation in ammonia compensation point and nitrogen pools in beech leaves (Fagus sylvatica), Plant Soil, 343, 51–66, doi:10.1007/s11104-010-0693-7, 2011.

Wyers, G. P. and Erisman, J. W.: Ammonia exchange over coniferous forest, Atmos. Environ., 32, 441–451, doi:10.1016/S1352-2310(97)00275-6, 1998.

Wyers, G. P., Vermeulen, A. T., and Slanina, J.: Measurement of Dry Deposition of Ammonia on a Forest, Environ. Pollut., 75, 25–28, doi:10.1016/0269-7491(92)90052-C, 1992.

Xiankai, L., Jiangming, M., and Shaofeng, D.: Effects of nitrogen deposition on forest biodiversity, Acta Ecologica Sinica, 28, 5532–5548, doi:10.1016/S1872-2032(09)60012-3, 2008.

Zhang, L., Wright, L. P., and Asman, W. A. H.: Bi-directional air-surface exchange of atmospheric ammonia: A review of measurements and a development of a big-leaf model for applications in regional-scale air-quality models, J. Geophys. Res.-Atmos., 115, D20310, doi:10.1029/2009JD013589, 2010.

Table 1. Statistics of the atmospheric ammonia (NH_3) flux measured above Lille Bøgeskov using relaxed eddy accumulation (33 m) in the period 21 October–15 November 2010.

	Mean ($\mu g\,NH_3\text{-}N\,m^{-2}\,s^{-1}$)	Min ($\mu g\,NH_3\text{-}N\,m^{-2}\,s^{-1}$)	Max ($\mu g\,NH_3\text{-}N\,m^{-2}\,s^{-1}$)	Uncertainty ($\mu g\,NH_3\text{-}N\,m^{-2}\,s^{-1}$)
NH_3 flux (F_{NH_3})	0.087	−0.33	0.96	0.006–0.491

Table 2. Atmospheric ammonia (NH_3) concentration [$\mu g\,NH_3\text{-}N\,m^{-3}$] conducted using relaxed eddy accumulation (REA) measurement technique (33 m), denuder measurements (29.8 m) and the DAMOS model for Lille Bøgeskov in the period 21 October–15 November 2010.

	Mean ($\mu g\,NH_3\text{-}N\,m^{-3}$)	Min ($\mu g\,NH_3\text{-}N\,m^{-3}$)	Max ($\mu g\,NH_3\text{-}N\,m^{-3}$)	Uncertainty ($\mu g\,NH_3\text{-}N\,m^{-3}$)	DL ($\mu g\,NH_3\text{-}N\,m^{-3}$)
REA (c_{RNH_3})	0.68	0	1.98	0.35	0.03
Denuder (c_{dNH_3})*	0.67	–	–	0.05	0.003
DAMOS (c_{mNH_3})	0.56	0.03	2.51	0.28	–

* c_{dNH_3} are only measured in the period 26 October–11 November.

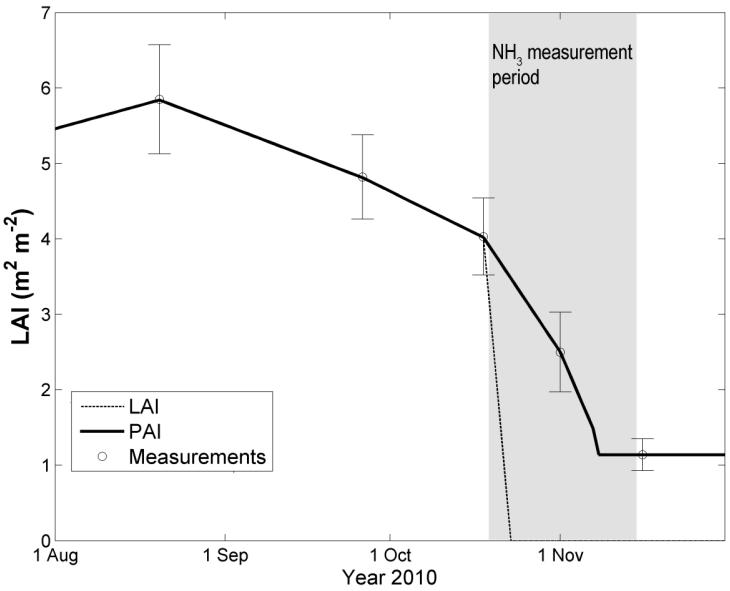

Fig. 1. Vegetation status of Lille Bøgeskov during autumn 2010 represented by plant area index (PAI) and leaf area index (LAI). Open circles show the LAI-2000 measurements of PAI with the standard deviations indicated by the error bars. Daily values of PAI (solid line) and of LAI (dotted line) are found from linear interpolation. The grey rectangular area shows the ammonia (NH_3) measurement period (21 October–15 November).

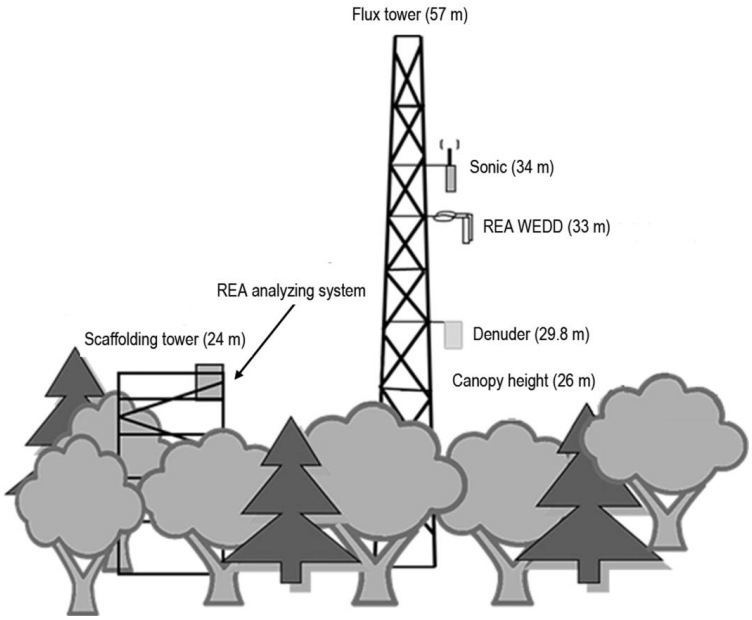

Fig. 2. Instrumental setup in Lille Bøgeskov for atmospheric ammonia (NH_3) measurements. A flux tower (57 m) is equipped with a sonic (34 m) to measure micro meteorological parameters, two Wet Effluent Diffusion Denuders (WEDDs) for the relaxed eddy accumulation (REA) system (33 m) and seven glass denuders (29.8 m) to measure atmospheric NH_3. The REA analysing system is located at the top floor of a scaffolding tower (24 m).

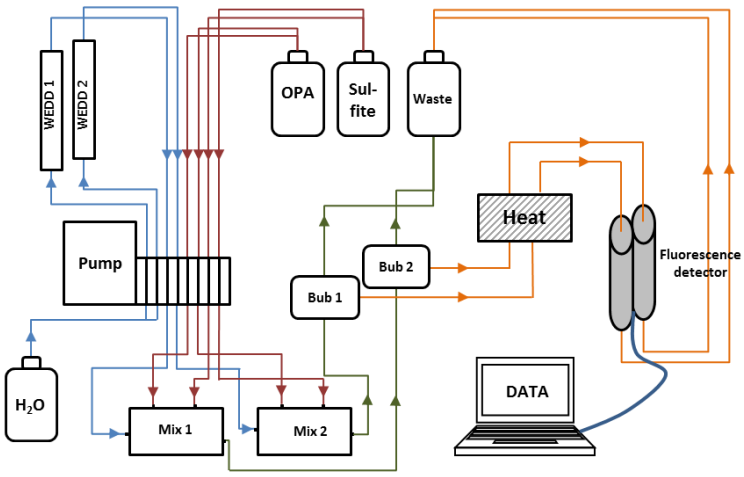

Fig. 3. Schematic overview of the relaxed eddy accumulation (REA) analysing system for NH_3 flux measurements. The path of the liquid mixture of NH_3 and H_2O through the Wet Effluent Diffusion Denuders (WEDDs) (one for updraft eddies of air and one for downdrafts) is indicated with the blue line, the mixing with the chemical reagents *o*-phthaldialdehyde (OPA) and sulphite with the red line, the path through the de-bubbler with green and finally through the heating coiler and fluorescence detector with yellow.

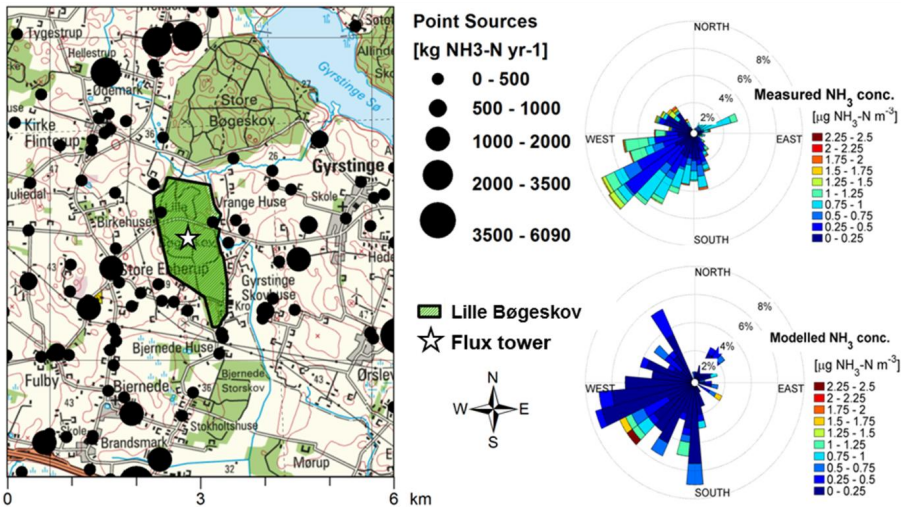

Fig. 4. NH_3 emissions (kg NH_3-N yr^{-1}) from point sources in 2008 (data are described in Sect. 2.6). The flux tower is marked with a white star in Lille Bøgeskov (the green scratched area). The concentration roses show measured concentration using REA (upper) and modelled concentration using DAMOS (lower) related to measured and simulated wind direction, respectively. Red colours indicate the highest assessed concentrations and blue indicate lowest concentrations.

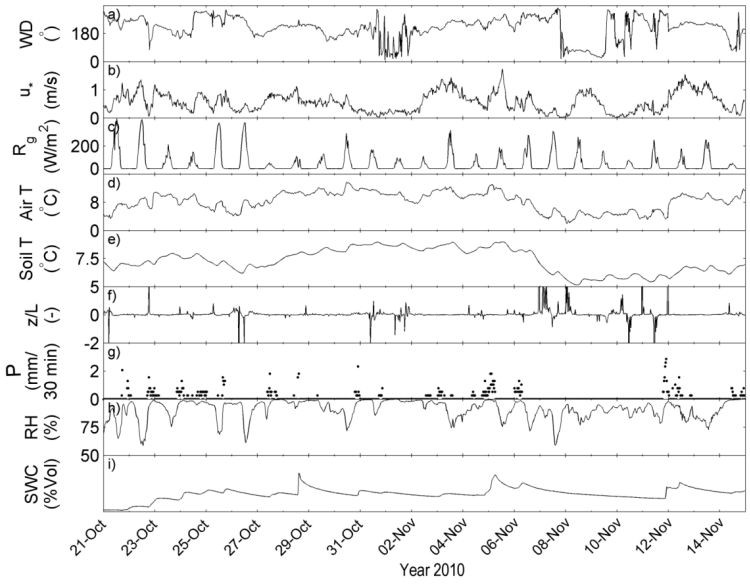

Fig. 5. Meteorological and soil measurements of **(a)** wind direction [°], **(b)** friction velocity [m s^{-1}], **(c)** global radiation [W m^2] **(d)** temperature [°C], **(e)** soil temperature [°C] **(f)** atmospheric stability (z/L), **(g)** precipitation [mm], **(h)** relative humidity [%] and **(i)** soil water content [%vol] for Lille Bøgeskov during 21 October to 15 November.

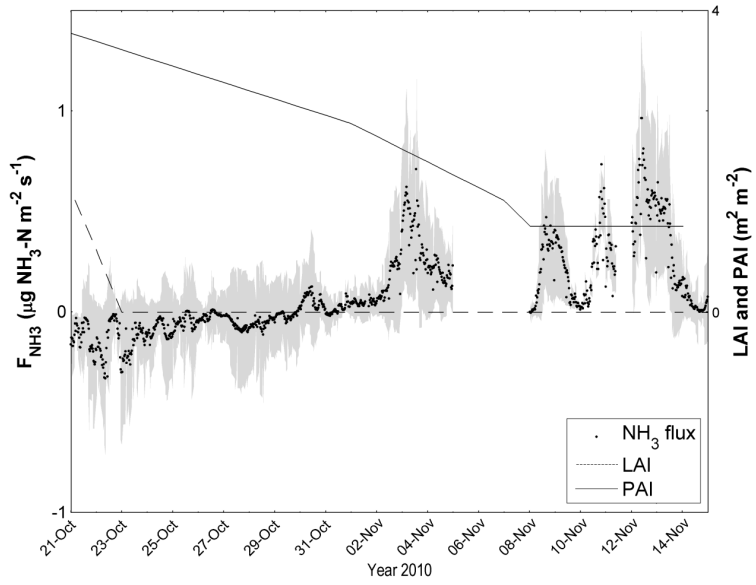

Fig. 6. Half-hourly mean NH_3 fluxes (black dots) for Lille Bøgeskov from 21 October–15 November 2010 measured using REA in 33 m height. Grey shadings indicate the measurement uncertainty. Leaf area index (LAI) and plant area index (PAI) are also indicated as a dashed and solid line, respectively.

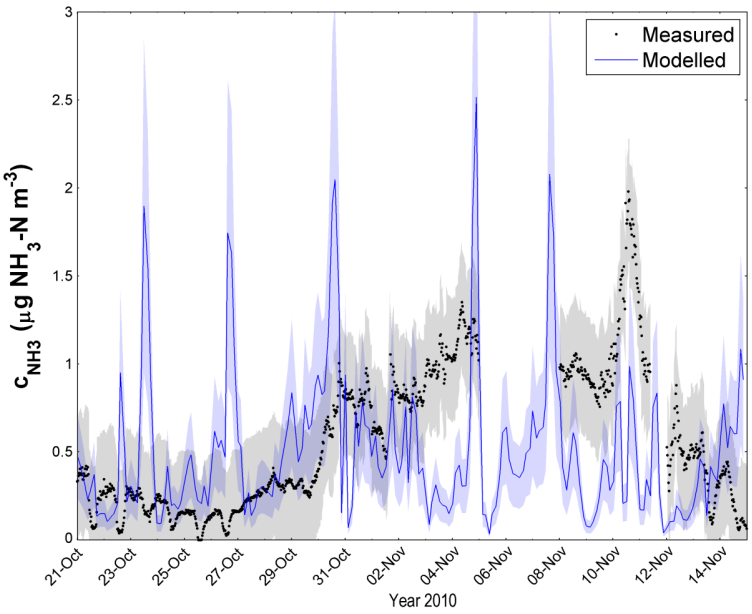

Fig. 7. Measured half-hourly mean NH_3 concentrations (black dots) using REA and modelled three-hourly mean NH_3 concentrations using DAMOS for Lille Bøgeskov from 21 October–15 November 2010. Grey shadings around the dots indicate the measurement uncertainty and blue shading the modelled uncertainty.